Journal of Materials Chemistry A

Accepted Manuscript

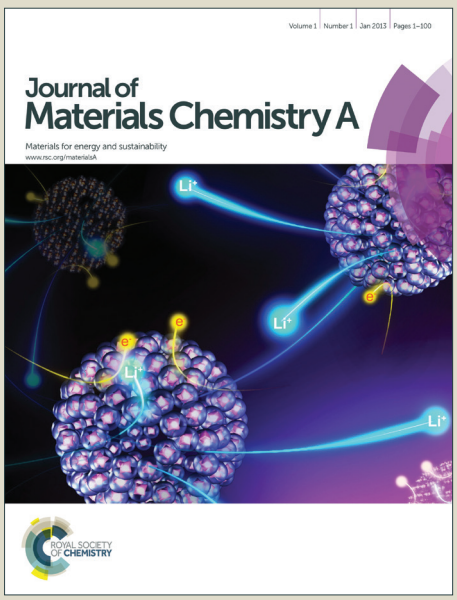

This is an *Accepted Manuscript*, which has been through the Royal Society of Chemistry peer review process and has been accepted for publication.

Accepted Manuscripts are published online shortly after acceptance, before technical editing, formatting and proof reading. Using this free service, authors can make their results available to the community, in citable form, before we publish the edited article. We will replace this *Accepted Manuscript* with the edited and formatted *Advance Article* as soon as it is available.

You can find more information about *Accepted Manuscripts* in the Information for Authors.

Please note that technical editing may introduce minor changes to the text and/or graphics, which may alter content. The journal's standard Terms & Conditions and the Ethical guidelines still apply. In no event shall the Royal Society of Chemistry be held responsible for any errors or omissions in this *Accepted Manuscript* or any consequences arising from the use of any information it contains.

ROYAL SOCIETY OF CHEMISTRY

www.rsc.org/materialsA

Journal of Materials Chemistry A RSCPublishing

ARTICLE

Improved Electrochemical Performance of $Li_{1.2}Mn_{0.54}Ni_{0.13}Co_{0.13}O_2$ by Mg-doping for Lithium Ion Battery Cathode Material

Cite this: DOI: 10.1039/xoxxoooooox

Received ooth January 2014,
Accepted ooth January 2014

DOI: 10.1039/xoxxoooooox

www.rsc.org/

Hongjie Xu,[a] Shengnan Deng[b] and Guohua Chen[a,b,*]

Li-rich Mn-based layered material has been considered to be one of the most promising cathode materials for next-generation lithium ion batteries. However, this material suffers from problems of severe capacity fading and poor rate capability. By partially replacing Li with Mg, the electrochemical performance of the material was found improved. Structural and elemental analyses indicate an expansion of the unit cell as a result of Mg doping, while the crystal structure remains unaffected. Higher specific capacity and better rate capability with more stable cycling performance are obtained from the sample of $Li_{1.17}Mg_{0.03}Mn_{0.54}Ni_{0.13}Co_{0.13}O_2$ than other samples either Mg-free or with Mg content beyond 0.03.

Introduction

Layered structure lithium transition metal oxide materials have been intensively investigated by various researchers in recent years since they generally provide higher specific capacity and higher voltage plateau against lithium than those of spinel or polyanion type cathodes. However, these materials suffered from the instability of crystal structure during lithium intercalation/deintercalation. In addition, the energy density and power density they deliver are still far from the requirements for next generation lithium ion batteries. Hence, lithium-rich materials are proposed to further improve the layered materials. Such an improvement was made by the introduction of Li_2MnO_3 phase which has high structural integration with layered oxide.[1] The resulting Li-rich Mn-based layered oxide that exhibits many attractive features like high capacity, high voltage plateau, and good thermal stability has been widely regarded as one of the most promising candidates for future electric vehicles (EV) industry.[2-4]

Up to date, these attractive features have only been realized to certain limit with a number of drawbacks remaining. One of these drawbacks lies on the unstable layer structure of Li-rich materials. There is a risk of rhombohedral lattice distorted into monoclinic one when lithium ions are deintecalated from the structure.[5] The situation becomes more serious when Li and O atoms are lost from the structure during first cycle charge. In order to maintain the structural stability, numerous approaches have been tested by introducing alien elements to tune the layered structure.[6-8] However, most of the researches focused on the replacement of transition metal Ni, Co or Mn. Replacement of Li could be another way to improve the stability of the structure. If the alien atoms introduced on Li sites can provide strong bonding with neighbouring oxygen atoms, especially after lithium ion depletion, the movement within the crystal structure during electrochemical reaction can possibly be confined.

It has been noticed that, in the high temperature synthesis of typical layered oxide such as $LiNiO_2$ and $LiNi_{1-x-y}Co_xMn_yO_2$, a cation mixing effect would occur due to the similarity on the radii between Li^+ (90 pm) and Ni^{2+} (83 pm).[9, 10] A certain amount of Ni^{2+} would locate in the lithium layer after calcinations, while some lithium atoms would occupy sites in the transition metal layers. This phenomenon suggests that it is possible to place the alien atoms at desired positions. To verify such a hypothesis, certain criteria should be applied to the candidate of alien cations. First of all, its ionic radius shall be close to that of Li^+ to make sure that it has preferential site in the lithium layer. Secondly, it should be electrochemically inert in order to prevent any variation to the structure. Thirdly, it would be better to have divalent ions to minimize the internal stress so as to avoid undesired distortion. Under such criteria, Mg^{2+} (86 pm) becomes a possible candidate to evaluate in the present study.

Experimental section

Sample preparation

Transition metal sulfates $MnSO_4 \cdot H_2O$ (Aldrich, 99%), $NiSO_4 \cdot 6H_2O$ (Aldrich, 99%) and $CoSO_4 \cdot 7H_2O$ (Aldrich, 99%), with molar ratio of 4:1:1 were dissolved into 100 ml de-ionized (DI) water to make a 1 M solution. In the meantime, Na_2CO_3 (BDH, 99.9%) was dissolved into another 100 mL DI water to prepare a 1 M solution. 1.8 mL of $NH_3 \cdot H_2O$ (Wako, 28% aqueous solution) was added into this solution. After that, two

Journal of Materials Chemistry A Accepted Manuscript

as-prepared solutions were added into 300 mL DI water respectively via peristaltic pump at a flow rate of 4 mL·min^{-1}. The mixed solution was kept under constant stirring for 12 hours while the temperature was maintained at 55^{o} C. The carbonate precipitation obtained after reaction was filtered and oven-dried at 80^{o} C overnight. For preparing final product, desired amounts of MgO (Fisher, 98%) and LiOH·H_2O (Aldrich, 98%) were mixed thoroughly with the as-prepared transition metal carbonate by grinding them in an agate mortar. Some 5% of extra LiOH·H_2O was added in order to compensate any loss of Li during high temperature sintering. The ground powder was subjected to calcinations at 900^{o} C for 12 hours and then allowed to cool down to room temperature.

Sample characterizations

The morphology of the materials were observed via a scanning electron microscope (SEM, JOEL 6300F). Crystal structures of the materials were examined by X-ray diffraction (XRD, Philips PW1830) equipped with a Cu Kα radiation source (wavelength of 1.540562 Å) and graphite monochromator. The compositions of the materials and oxidation states of elements were measured via X-ray photoelectron spectroscopy (XPS, Kratos Axis Ultra DLD) with an Al anode source operating at an applied power of 150 W. C 1s peak was calibrated to 285.0 eV for each set of data before comparison. The compositions of samples were analyzed by an inductively coupled plasma optical emission spectroscopy (ICP-OES, Perkin Elmer Optima 7300DV).

Electrochemical measurement

The electrochemical performances of the cathodes were evaluated using CR2025 coin-type cells. Electrodes for electrochemical evaluation were prepared with 1-methyl-2-pyrrolidone (NMP) (Aldrich, 99% purity) slurry of active materials, polyvinylidene fluoride (PVdF), and acetylene carbon black in the wt. % ratio of 8:1:1. Lithium foils were used as counter electrodes, with a Celgard 2325 micro-porous polypropylene/polyethylene/polypropylene tri-layer membrane serving as separator. Some 1 M $LiPF_6$ dissolved in ethylene carbonate/dimethyl carbonate (3:7, v/v) was used as electrolyte. Electrochemical cells were assembled in a glove box (MBraun Labstar) filled with high purity argon. The as-prepared battery coin cells were used for galvanostatic charge-discharge test using battery testing system (Neware CT-3008W). There were at least two replicates for each test and only repeatable results were analyzed. Electrochemical impedance spectroscopy (EIS, Autolab PGSTAT100) were performed by applying an AC voltage of 5 mV in the frequency range from 1 MHz to 1 mHz. Each cell was allowed to relax for 12 hours once it was charged to 4.0 V before characterization.

Results and discussion

Morphology observation

SEM images reveal a typical particulate morphology for all the as-prepared samples (Figure 1). The sizes of particles vary from several hundred nanometers to about one micrometer. No visible morphology change can be found associated with Mg contents, indicating that the introduction of Mg would have insignificant impact on the growth of crystals or particles. Due to the small size, the particles tend to aggregate. This may not be desirable since it would reduce the surface area of the material.

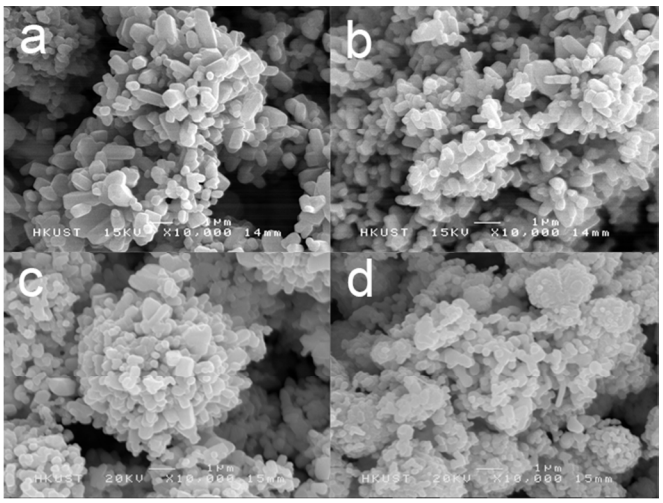

Figure 1. SEM images of $Li_{1.2-x}Mg_xMn_{0.54}Ni_{0.13}Co_{0.13}O_2$ samples with (a) x = 0; (b) x = 0.03; (c) x = 0.07; (d) x = 0.10. The scale bar = 1μm.

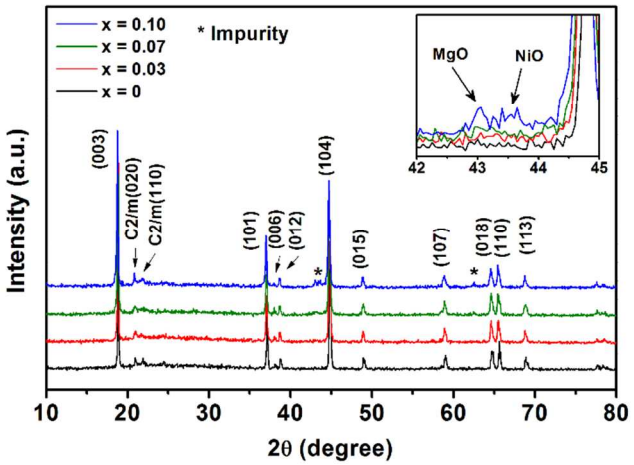

Figure 2. XRD patterns of $Li_{1.2-x}Mg_xMn_{0.54}Ni_{0.13}Co_{0.13}O_2$. Inset graph is the magnified plots ranged from 42^{o} to 45^{o}.

Structural analysis

Figure 2 shows the XRD pattern for samples with x = 0, 0.03, 0.07, and 0.10 in $Li_{1.2-x}Mg_xMn_{0.54}Ni_{0.13}Co_{0.13}O_2$. The peaks appear in all samples can be perfectly indexed according to hexagonal $R\bar{3}m$ symmetry. The minor peaks appearing at 2θ from 21 to 25^{o} show the signature of Li-rich material, which is due to the incorporation of $C2/m$ Li_2MnO_3 phase. The well-separated (018) and (110) peaks in all samples imply a good hexagonal ordering.[11] The Mg introduction into the compound leads to insignificant change in XRD patterns. Impurity peaks

Journal of Materials Chemistry A Accepted Manuscript

This journal is © The Royal Society of Chemistry 2014

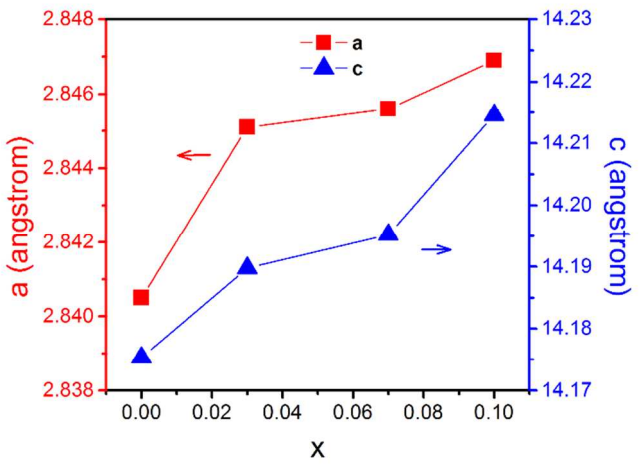

Figure 3. Lattice Parameters Calculated from XRD patterns.

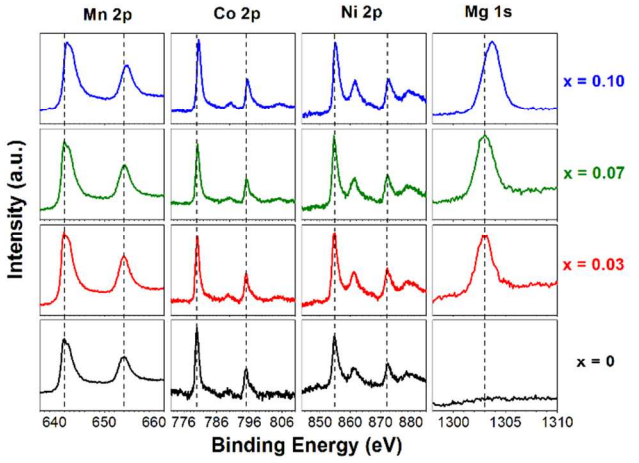

Figure 4. XPS spectra of Mn, Co, Ni and Mg in $Li_{1.2-x}Mg_xMn_{0.54}Ni_{0.13}Co_{0.13}O_2$.

at 42.5-44° and 62-63° are only visible when x = 0.10, as shown in the inset graph. They can be attributed to the impurities from MgO (JCPDS No. 89-7746) and NiO (JCPDS No. 89-7101), respectively. The former is derived from the unreacted raw material MgO. The latter is formed probably due to preferential occupation of Mg ions on the Ni site[12]. Such repelling effect on the Ni ions is magnified with the increase in Mg concentration. This result suggests that x = 0.10 is already excessive for Mg-doping.

Lattice parameters of crystal structure for all the samples are calculated from XRD spectrum using least-square method according to $R\bar{3}m$ symmetry. The data are plotted in Figure 3. The parameters *a* and *c* defined according to the hexagonal crystal system imply the size of transition metal-oxygen slab and inter-spacing of transition metal layers. There is an obvious trend that both parameters are increased along with the increase in Mg concentration. The values of *a* and *c* increase from 2.8405 and 14.1753 to 2.8469 and 14.2146 Å as x increases from 0 to 0.10. The ratio of these increments for *a* and *c* are 0.23% and 0.28%, respectively, which are nearly proportional. The increase of both cell parameters implies that Mg has enlarged the lattice of the crystal structure. This is reasonable since the length of Mg-O bonding in layered oxide is larger than that of Ni-O.[12]

Table 1. Chemical Compositions Acquired with ICP-OES Analysis

Sample	Normalized Element Content (Use Mn = 0.54 in all samples)				
	Li	Ni	Co	Mn	Mg
Precursor Carbonate	-	0.135	0.136	0.540	-
x = 0	1.234	0.140	0.139	0.540	-
x = 0.03	1.192	0.138	0.138	0.540	0.030
x = 0.07	1.161	0.136	0.138	0.540	0.069
x = 0.10	1.125	0.134	0.134	0.540	0.092

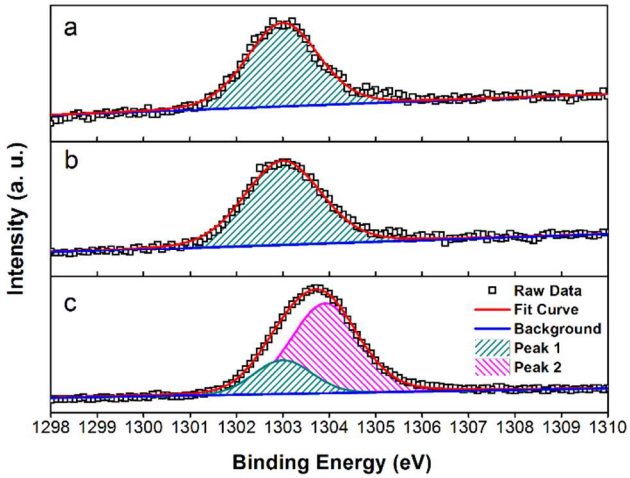

Figure 5. Fittings of Mg 1s XPS spectra for (a) x = 0.03; (b) x = 0.07 and (c) x = 0.10 samples in $Li_{1.2-x}Mg_xMn_{0.54}Ni_{0.13}Co_{0.13}O_2$.

The ICP-OES result is listed in Table 1. The concentration of each element is normalized by fixing the molar concentration of Mn in each sample at 0.54. The concentration of Mg in each sample can be seen in good agreement with the nominal stoichiometry. The concentration of transition metal is not affected significantly by the presence of Mg. The molar ratio values among Mn, Ni and Co are consistent with those in precursor carbonates precipitation before calcination. In contrast, the Li content is decreased with increasing Mg as expected.

The oxidation states of metal elements are examined by XPS, as illustrated in Figure 4. General observation does not reveal any significant change on the chemical states of elements when x is increased from 0 to 0.07, implying that the transition metal layers are quite stable in this range. However, when x is further increased to 0.10, the peaks of Mg shifted slightly to the higher binding energy. This phenomenon deserves more detailed study. Figure 5 shows the fitting of the spectra for Mg.

Journal of Materials Chemistry A Accepted Manuscript

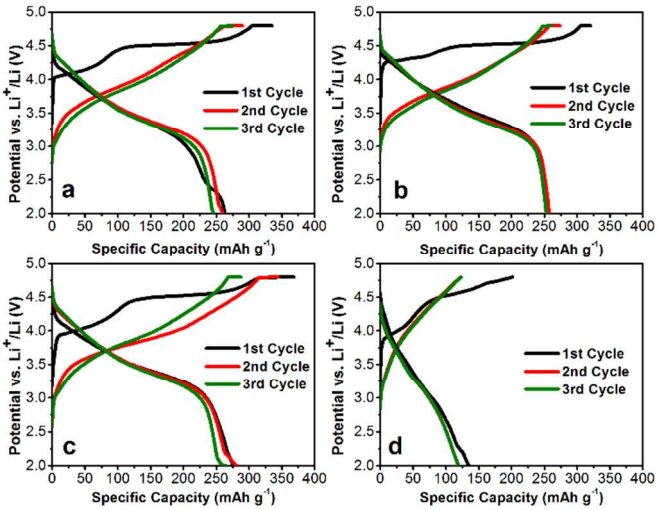

Figure 6. Charge-discharge profiles for first three cycles of cells made of $Li_{1.2-x}Mg_xMn_{0.54}Ni_{0.13}Co_{0.13}O_2$ with (a) x = 0; (b) x = 0.03; (c) x = 0.07; (d) x = 0.10.

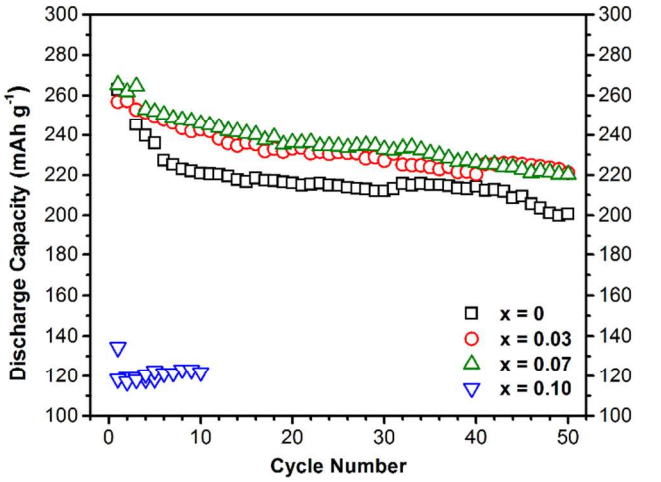

Figure 7. Discharge capacity of the cells with respect to cycle number under 0.1C for $Li_{1.2-x}Mg_xMn_{0.54}Ni_{0.13}Co_{0.13}O_2$.

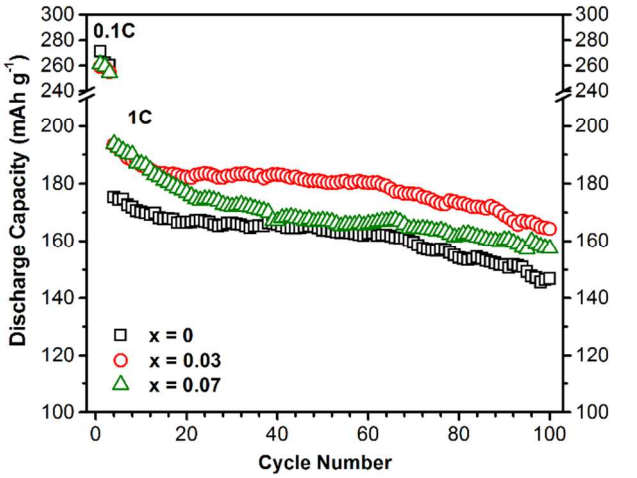

Figure 8. Discharge capacity of the cells with respect to cycle number under 1C for $Li_{1.2-x}Mg_xMn_{0.54}Ni_{0.13}Co_{0.13}O_2$.

For the two samples with lower concentrations of Mg, their Mg peaks can be well fitted using a single binding energy equal to 1303.0 eV. However, the fitting for the spectrum of the sample of x = 0.10 requires two binding energies, one at 1303.0 eV and the other at 1303.9 eV. The higher binding energy peak can be attributed to MgO[13], consistent with XRD results found from unreacted MgO. The peaks at 1303.0 eV can be attributed to the Mg-O bonding formed in the crystal lattice of the material, in agreement with what has been observed in Mg-doped layered oxide.[14] A lower value on the binding energy suggests that the electron density around Mg ions is increased, most likely due to the inductive effect of the surrounding ions or of local distortion at Mg sites.

Electrochemical performance

The charge-discharge profiles of the first three cycles for different samples are plotted in Figure 6, under a current density corresponding to 0.1 C (1 C = 200 mAg^{-1}). The first cycle charge and discharge profiles of these four samples show a typical Li_2MnO_3-integrated characteristic, i.e., a voltage plateau at about 4.5 V during charging, which is related to the oxygen loss, as discussed previously. All samples, except that of x = 0.10, could deliver first cycle charge capacity above 300 $mAhg^{-1}$, with following discharge capacity of about 250-260 $mAhg^{-1}$. The sample of x = 0.10 however shows a much lower capacity of 201 $mAhg^{-1}$ for charge and 134 $mAhg^{-1}$ for discharge. The first cycle efficiencies of these four samples are 78.7, 80.2, 72.1 and 66.7%, respectively. The following second and third cycles show a typical solid-solution profile, with the specific capacity remaining nearly at the same level in all samples, indicating a good electrochemical reversibility at initial state. The over-doping of Mg has an obvious negative impact on the electrochemical performance of the material. This impact is further illustrated by the battery cells cycling for 50 times at 0.1 C (Figure 7). The sample of x = 0 delivers a discharge capacity of about 260 $mAhg^{-1}$ in the first three cycles, followed by a quicker decay to only 200 $mAhg^{-1}$ after 50 cycles, while the samples with x = 0.03 and 0.07 exhibit a relatively better stability of over 220 $mAhg^{-1}$ capacity, 10% larger than the undoped one. The sample of x = 0.10, however, shows a much poorer performance, with merely 120$mAhg^{-1}$ found after 10 cycles. Therefore, further investigations will be carried out on the three samples of x = 0, 0.03 and 0.07 without considering x = 0.10.

The battery cells are tested for cycling under a higher current density of 1C after 3 cycles of activation under 0.1 C. The material with x = 0.03 shows a generally better stability than either the one of x = 0 or 0.07 samples (Figure 8). The specific capacity values after 100 cycles under 1 C are approximately 146, 164 and 157 $mAhg^{-1}$ for x = 0, 0.03 and 0.07 samples, respectively. EIS tests at different cycles (Figure S1) suggest that, with Mg doping, samples show larger charge transfer resistance initially. However, after 10th cycle, the x =

Journal of Materials Chemistry A Accepted Manuscript

This journal is © The Royal Society of Chemistry 2014

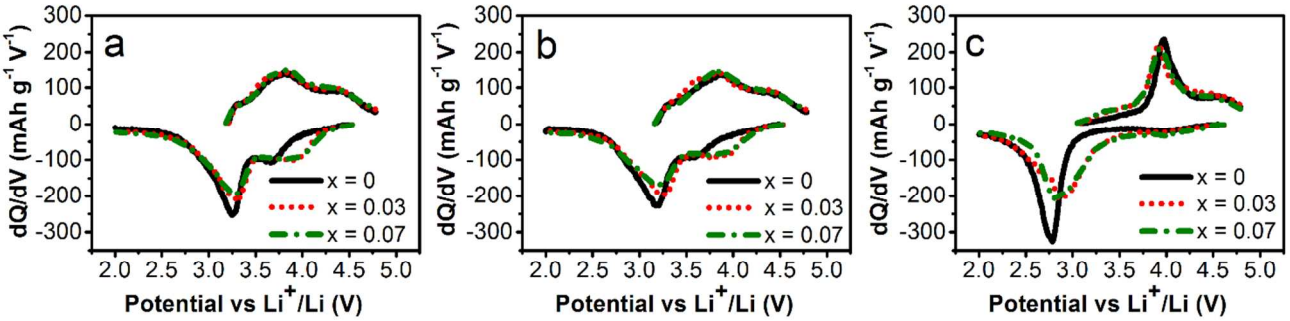

Figure 9. dQ/dV-V plots calculated based on the charge-discharge profiles at (a) 5th; (b) 20th; (c) 100th cycle under 1C for $Li_{1.2-x}Mg_xMn_{0.54}Ni_{0.13}Co_{0.13}O_2$.

0.03 sample has a lower resistance than the one without Mg. This trend is maintained up to 100 cycles. On the contrary, the sample with x = 0.07 shows a rapid increase in charge transfer resistance from 10th to 100th cycle. This EIS development is consistent with the much faster capacity decay observed from Figure 8 for x = 0.07 sample.

The dQ/dV-V plots calculated based on the charge-discharge profiles are illustrated in Figure 9. The curves representing the charge process, i.e., oxidation reaction at the $Li_{1.2-x}Mg_x Mn_{0.54}Ni_{0.13}Co_{0.13}O_2$ electrode, are basically the same for all three samples. Three broad peaks observed are located at 3.31, 3.84 and 4.39 V, respectively. In the following discharge process, two peaks can be observed at 3.96 and 3.28 V for samples with x = 0.03 and 0.07. For the x = 0 sample, a peak around 3.28 V can be seen. However, the second peak at high voltage shifts significantly to lower value of 3.66 V. This shift can be easily seen again when the cells are further cycled up to 20 cycles (Figure 9b). The oxidation peaks at 3.84 and 4.39 V, and the corresponding reduction peak at 3.96 V can be attributed to the redox reaction of Ni and Co, similar to that observed from the commonly studied $LiMn_{0.33}Ni_{0.33}Co_{0.33}O_2$ material[15]. The redox pair below 3.5 V, which is the characteristic of Li-rich material, should be derived from the structural rearrangement after the first cycle oxygen loss. The change of reduction peak from originally 3.66 V in pristine sample to 3.96 V in Mg-doped sample implies that the introduction of Mg has modified the local environment around the transition metal ions and elevated the voltage, which is in agreement with the XPS results. After 100 cycles, the peaks originally located at 3.31 and 4.39 V in the charge process become indiscernible. Instead, one sharp peak located around 3.9 V, very close to original 3.84 V, can be observed. Similarly for the discharge process, only one significant peak around 2.7-2.8 V is found instead of the originally visible 3.96 and 3.28 V peaks (Figure 9c).

The change on the peak positions implies a structural transformation during cycling, since the redox potentials are related to the chemical potential of Li ions. This transformation is generally considered as change from layered to spinel-like structure. The oxidation peak at 3.9 V and reduction peak at 2.8 V can be attributed to the insertion and depletion of Li ions from tetrahedral sites and octahedral sites, respectively.[16] The absence of corresponding reduction peak around 3.9 V and oxidation peak around 2.7 V indicates a hopping process of Li ions from octahedral sites to tetrahedral sites upon cycling. More specifically, Li ions are firstly removed from tetrahedral sites in charge process, while Li ions at neighbouring octahedral sites hop into the vacant tetrahedral sites to compensate and maintain the structural stability. Upon discharge, Li ions are inserted to the vacant octahedral sites. This hopping mechanism has found support from the NMR observation[17] and theoretical calculation[18]. It should be mentioned that the size of the crystal lattice has a strong impact on this hopping process. As shown in XRD analysis (Figure 3), the lattice sizes of Mg-doped samples are larger than that of pristine sample, which may facilitate this hopping. This facilitation is also reflected by the narrowed differences between the oxidation and reduction peaks in these two Mg-doped samples than the one in Mg-free sample. Thus, one can expect the rate performance of Mg-doped samples improved.

The performances of battery cells under different current density are presented in Figure 10. The cells are charged with a current density of 0.2 C (40 mAg^{-1}) before each discharge. The

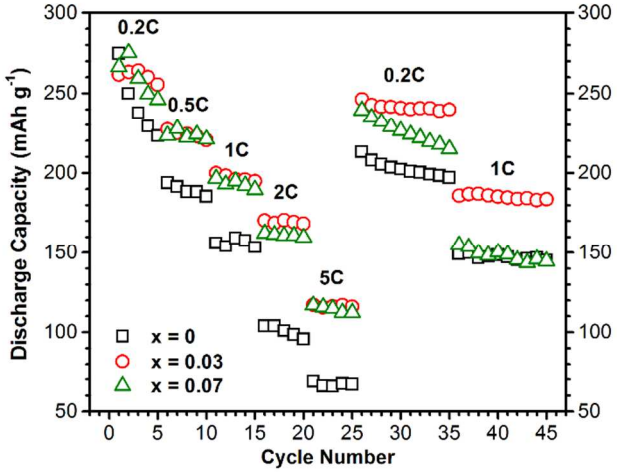

Figure 10. Discharge capacity of the battery cells under different current density for $Li_{1.2-x}Mg_xMn_{0.54}Ni_{0.13}Co_{0.13}O_2$.

Journal of Materials Chemistry A Accepted Manuscript

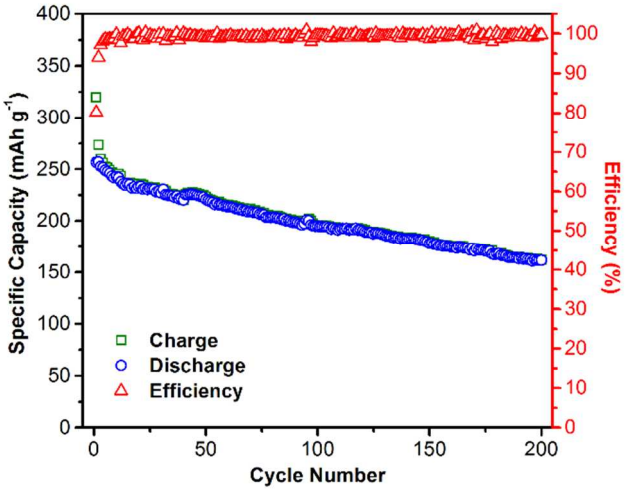

Figure 11. Cycling performance of cell made of sample with x = 0.03 under 0.1C.

capacity obtained at all current rate for Mg-doped samples is much higher than the one for pristine sample, implying that the existence of Mg indeed enhanced the transportation of Li ions. It should be noted that there is a serious fading on the capacity for x = 0.07 sample when the current density is decreased from 5 to 0.2 C. Further cycling at 1 C rate displays a relatively lower capacity than the one of x = 0.03 sample. Recall that similar capacity fading and resistance increasing appear for x = 0.07 sample during 1 C cycling. This phenomenon may suggest that the sample become unstable at high current density. One possible reason behind this fading is that over-doping of Mg jeopardizes the stability of the crystal structure. Moreover, trace amount of insulating MgO could still exist, although it has not been identified by XRD or XPS because of the detecting limits of such instruments.

In general, the sample with x = 0.03 shows relatively higher capacity, rate capability and better stability. This effect can be further illustrated by cycling the battery cells up to 200 cycles with current density of 0.1 C (Figure 11). The material retains capacity at 195 $mAhg^{-1}$, about 76% of the original value, after 100 cycles. The percentage capacity retention is 63% up to 200 cycles, or 162 $mAhg^{-1}$ in terms of discharge capacity.

It should be mentioned that, although theoretically it is preferential for Mg ions to occupy Li sites, it becomes complicated in practice since the mobility of different ions as well as the redox reaction play crucial roles in defining the eventual structure during synthesis of materials. The location of Mg ions become even more unclear when the cations migration during electrochemical reaction[19] is taken into account. The exact position of Mg ions inside the structure therefore remains an open question which unfortunately neither the results from XRD nor XPS can answer. In addition, the electrochemical performance is indeed improved by altering the concentration of Li and Mg instead of transition metals. The detail mechanism behind this improvement is still vague. A possible explanation is that, with the existence of supervalent Mg ions, some crystalline defects and vacancies will form, which may lead to the increase in the conductivity, as supported by the EIS results. Given that the cations are migrating during the charge-discharge process, the materials could end up glassy, in which Mg ions could act as a modifier and facilitate the Li ion diffusion. Further studies are therefore necessary to address this issue more satisfactorily.

Conclusions

$Li_{1.2-x}Mg_xMn_{0.54}Ni_{0.13}Co_{0.13}O_2$ materials are successfully synthesized. The structural analysis reveals that, Mg is introduced by means of substituting Li ions, which results in the expansion of the lattice. Such an expansion is beneficial to the electrochemical performance of the material in terms of capacity and rate capability. In the meantime, the substitution of Li by Mg led to the structural stabilization of the material, showing a better cycling performance, especially under high current density. Experimental data show that x = 0.03 is an ideal amount of Mg doping, while over-doping of Mg may lead to an unstable structure of material and undesired impurities, which eventually causes poor electrochemical performance of the battery cells.

Acknowledgements

The authors gratefully acknowledge the financial supports from HK Innovation and Technology Commission under GHP/033/08SZ, School of Engineering Research Excellence Fund, HKUST-SBI11EG13, and HKUST Seed Research Fund Initiative SRFI11EG17PG-A under the title of "Sustainable energy: production and storage". We are very grateful of comments and suggestions from Professor Jean-Marie Tarascon for the revision of the manuscript.

Notes and references

[a] Department of Chemical and Biomolecular Engineering, The Hong Kong University of Science and Technology, Hong Kong, China.
[b] Centre for Green Products and Processing Technologies, Guangzhou HKUST Fok Ying Tung Research Institute, Guangzhou, China.
* Corresponding author, email: kechengh@ust.hk .
Electronic Supplementary Information (ESI) available: [EIS results for $Li_{1.2-x}Mg_xMn_{0.54}Ni_{0.13}Co_{0.13}O_2$]. See DOI: 10.1039/b000000x/

1. M. M. Thackeray, S.-H. Kang, C. S. Johnson, J. T. Vaughey, R. Benedek and S. A. Hackney, *J Mater Chem*, 2007, 17, 3112-3125.
2. Z. H. Chen, D. J. Lee, Y. K. Sun and K. Amine, *MRS Bulletin*, 2011, 36, 498-505.
3. V. Etacheri, R. Marom, R. Elazari, G. Salitra and D. Aurbach, *Energ Environ Sci*, 2011, 4, 3243-3262.
4. R. Marom, S. F. Amalraj, N. Leifer, D. Jacob and D. Aurbach, *J Mater Chem*, 2011, 21, 9938-9954.
5. M. E. Arroyo y de Dompablo and G. Ceder, *J Power Sources*, 2003, 119-121, 654-657.
6. S. H. Kang and K. Amine, *J Power Sources*, 2003, 119-121, 150-155.
7. N. Yabuuchi, K. Yamamoto, K. Yoshii, I. Nakai, T. Nishizawa, A. Omaru, T. Toyooka and S. Komaba, *J Electrochem Soc*, 2012, 160, A39-A45.

Journal of Materials Chemistry A Accepted Manuscript

This journal is © The Royal Society of Chemistry 2014

8. D. Wang, Y. Huang, Z. Huo and L. Chen, *Electrochim Acta*, 2013, 107, 461-466.
9. N. Yabuuchi and T. Ohzuku, *J Power Sources*, 2003, 119, 171-174.
10. Y. Koyama, I. Tanaka, H. Adachi, Y. Makimura and T. Ohzuku, *J Power Sources*, 2003, 119-121, 644-648.
11. X. Y. Zhang, W. J. Jiang, A. Mauger, Qilu, F. Gendron and C. M. Julien, *J Power Sources*, 2010, 195, 1292-1301.
12. K. Tatsumi, Y. Sasano, S. Muto, T. Yoshida, T. Sasaki, K. Horibuchi, Y. Takeuchi and Y. Ukyo, *Phys Rev B*, 2008, 78.
13. H. Seyama and M. Soma, *J Chem Soc Farad T 1*, 1984, 80, 237-248.
14. E. Zhecheva, R. Stoyanova, G. Tyuliev, K. Tenchev, M. Mladenov and S. Vassilev, *Solid State Sci*, 2003, 5, 711-720.
15. J. Wilcox, S. b. Patoux and M. Doeff, *J Electrochem Soc*, 2009, 156, A192.
16. R. J. Gummow and M. M. Thackeray, *J Electrochem Soc*, 1994, 141, 1178-1182.
17. C. P. Grey, W.-S. Yoon, J. Reed and G. Ceder, *Electrochemical and Solid-State Letters*, 2004, 7, A290.
18. K. Kang and G. Ceder, *Phys Rev B*, 2006, 74, 094105.
19. N. Yabuuchi, K. Yoshii, S. T. Myung, I. Nakai and S. Komaba, *J Am Chem Soc*, 2011, 133, 4404-4419.

Journal of Materials Chemistry A Accepted Manuscript